Eur. Phys. J. Special Topics **224**, 319–340 (2015)

DOI: 10.1140/epjst/e2015-02363-5

THE EUROPEAN PHYSICAL JOURNAL SPECIAL TOPICS

Review

# Surface waves in thermocapillary flow–revisited

C. Bach and D. Schwabe[a]

Physikalisches Institut der Justus-Liebig-Universitaet, Giessen, Germany

Received 25 July 2014 / Received in final form 16 February 2015
Published online 8 April 2015

**Abstract.** Following theoretical predictions [1,2] thermocapillary layers can exhibit instabilities called "hydrothermal waves" (HTWs) and "surface waves" (SWs) at sufficiently large Marangoni numbers. Only two experiments on thermocapillary layers in annular gaps describe SWs until now whereas HTWs have been found and investigated many times. We review and complement the results on SWs in thermocapillary annular gaps which are in fair agreement with theory, though severe differences between experimental and theoretical boundary conditions exist. Surface waves exhibit a considerably larger frequency, phase speed and surface deformation-amplitude compared to HTWs. The critical Marangoni numbers of the SWs are larger than those of the HTWs for layer depth $d < 1.7\,\mathrm{mm}$ at which depth they cross over. SWs and HTWs are found to coexist for a certain range of liquid depths at supercritical Marangoni numbers. Surprisingly, thermocapillary instabilities of the type of SWs can exist in the liquid meniscus at the cold end-wall in an underfilled cuvette with buoyant-thermocapillary convection and they can excite standing gravity surface waves under resonance conditions. These conditions are the underfilling of the cuvette (the meniscus shape) and the temperature difference between the end-walls. Experimental evidence for this complex phenomenon is presented.

## 1 Introduction

Thermocapillary forces drive flow by surface tension differences where the latter are due to temperature differences in the free surface of liquids with temperature-dependent surface tension. This type of force is abundant in technological processes. The coupling of themocapillary forces with buoyancy forces is always present at normal gravity, however, thermocapillary forces can well dominate in layers of only a few millimetre thickness d. This situation was studied by Smith and Davis [1,2] in a theoretical model; (i) infinitely extended layer, (ii) linear thermocapillary flow with "return flow", (iii) constant temperature gradient imposed in x-direction along the layer, (iv) gravity g=0. Two different conditions for the flexibility of the free surface have been investigated, namely (a) the inflexible surface and (b) the flexible surface, characterized by the surface tension parameter $S = \rho\, d\, \sigma \mu^{-2}$ with density $\rho$, layer thickness d, mean surface tension $\sigma$ and viscosity $\mu$. The non-deformable free surface is represented by $S \to \infty$. The driving force of the flow is characterized by the

[a] e-mail: Dietrich.Schwabe@physik.uni-giessen.de

**Table 1.** Relevant physical properties of ethanol at 20°C.

| Property of ethanol | Value at 20°C | Dimension |
|---|---|---|
| Density $\rho$ | **789.4** | $\mathrm{kg\,m^{-3}}$ |
| Temperature coefficient $\mathrm{d}\rho/\mathrm{dT}$ | **−0.84** | $\mathrm{kg\,m^{-3}\,K^{-1}}$ |
| Surface tension $\sigma$ | **22.75** | $\mathrm{N\,m^{-1}}$ |
| Temperature coefficient $\mathrm{d}\sigma/\mathrm{dT}$ | **−0.09** | $10^{-3}\,\mathrm{N\,m^{-1}K^{-1}}$ |
| Specific heat $\mathrm{c_p}$ | **2414** | $\mathrm{J\,kg^{-1}\,K^{-1}}$ |
| Thermal conductivity $\lambda$ | **0.166** | $\mathrm{J\,m^{-1}\,sec^{-1}\,K^{-1}}$ |
| Thermal diffusifity $\chi$ | **8.7** | $10^{-8}\,\mathrm{m^2\,sec^{-1}}$ |
| Dynamic viscosity $\eta$ | **1.20** | $10^{-3}\,\mathrm{kg\,m^{-1}\,sec^{-1}}$ |
| Kinematic viscosity $\nu$ | **1.52** | $10^{-6}\,\mathrm{m^2\,sec^{-1}}$ |
| Vapour pressure | **5700** | $\mathrm{N\,m^{-1}}$ |
| Prandtl number Pr | **17** | |
| Surface tension number $\mathrm{S} = \mathrm{d}\rho\sigma/\mu^2$ for a layer thickness $\mathrm{d} = 1\,\mathrm{mm}$ | $5.73\ 10^3$ | |

Reynolds number $\mathrm{R} = \rho\gamma\,\mathrm{bd}^2\,\mu^{-2}$, with the negative value of the temperature dependence of the surface tension $\gamma$ and the temperature gradient b. The Marangoni number is given by $\mathrm{Ma} = \mathrm{R\ Pr}$ where Pr is the Prandtl number.

### 1.1 The inflexible free surface and hydrothermal waves

It is rather non-realistic to assume a totally non-deformable free liquid surface besides the other restrictions (i) to (iii) mentioned above, however, the simplified model problem could be treated by three-dimensional linear stability analysis. For these assumptions the instability in the form of hydrothermal waves (HTWs) was predicted to occur at elevated Marangoni number Ma and its features have been calculated [1]. We can cite only a selected number of experiments on HTW-like instabilities in thermocapillary liquid bridges which address the wavy nature of the instability [3–14] and in thin liquid layers [15–29] which have been performed in the meantime. All experiments displayed comparable results to the prediction of the theory of Smith & Davis. These HTWs can travel under a certain angle to the temperature gradient, either upstream or downstream, depending on the Prandtl number Pr of the liquid [1,4] and possible geometrical constraints. In contrast to the condition of an inflexible interface for the theoretical HTWs many experimenters observed in the time-dependent state of their experiment faint, but distinct regular oscillations of the free surface with the frequency of the HTWs (e.g. when observing the free surface under the glancing angle). It is agreed on, that these faint surface oscillations are merely passive reactions of the free surface on the HTW, be it on the flow pressure oscillations or on temperature oscillations. They have no influence on the HTW.

### 1.2 The flexible free surface and surface waves

In a following paper Smith & Davis [2] allowed for a flexible free liquid surface and conducted a two-dimensional linear stability analysis. The value of the surface tension parameter S of typical experimental liquids is between $\mathrm{S} = 10^4$ and $\mathrm{S} = 10^3$. The S of our experimental liquid ethanol is $5.73\,10^3$ (Table 1) and the results of the analysis of Smith & Davis seem to be applicable to our experiments. They found travelling waves that couple surface deflections with the underlying bulk shear flow. These waves are

closely related to the instabilities sustained by isothermal liquid layers subject to wind stresses [2] and they do not depend on the thermal boundary conditions at the surface and, especially not on those at the bottom of the liquid layer. This point is important in connection with one of our experiments. Such waves have been observed as well in experiments with lid-driven cavity-flow with deformable surface [30]. Thus the imposed temperature gradient and consequent surface tension gradient drive the basic shear flow but have little effect on the surface wave instabilities. We call this instability "Surface Waves (SWs) driven by thermocapillary flow". It is the aim of the present paper to discuss and to complement the few available experimental results on SWs in side-heated thin liquid layers in the light of the paper by Smith & Davis. The liquid in all discussed experiments is ethanol with a Prandtl number Pr = 17. We can find in the theoretical paper of Smith & Davis only indications of the critical conditions for the SWs in thin layers of ethanol (Smith & Davis concentrated on low Prandtl liquids) and we have to discuss the limitations and restriction of experiments in comparison with theory. We discuss the question why the SWs have been only seldom observed in contrast to the frequent reports on HTWs.

### 1.3 The liquid meniscus at the cold end-wall and surface waves

Besides in thin flat layers, thermocapillary instabilities can as well develop in the curved liquid meniscus at the cold end-wall of a side-heated cuvette. We present one new and surprising effect of the SWs; this is the resonance of faint surface oscillations of the SWs in the liquid meniscus at the cooled sidewall with macroscopic standing gravity surface waves (SGSWs) in an under-filled rectangular side-heated cuvette. The SGSWs found in this experiment can be excited and sustained by the action of the SWs in the liquid meniscus at the cold end-wall of the cuvette. The assignment of the effect to SWs is tentative.

## 2 Surface waves in thermocapillary liquid layers after the theory of Smith & Davis

We summarize the results from Smith & Davis [2] which are relevant for our experiments. The layer is again infinite in x-direction, bounded below by an adiabatic bottom (no heat flux). It is important to note that our experimental liquid layers have finite length L and are bounded at the hot and at the cold end by solid end-walls. The aspect ratio is $A = d/L$. The free interface is located at $z = 1 + \eta(x, t)$ allowing for significant deflections. The authors take into account that on the free surface the normal stress balances the surface tension times curvatures, and that the tangential stress balances the gradient of surface tension along the interface. The bounding gas is passive with constant pressure taken equal to zero.

The authors consider the parallel flow solution (surface flow with its return flow) as for the case with the non-flexible interface where they found HTWs and applied infinitesimal two-dimensional disturbances. They linearized their system of governing equations and arrived at solvable linear disturbance equations after some justified approximations. They treated first "the inviscid problem for the linear flow"(surface flow without return flow). This is not our case of thermocapillary flow in side-heated layers, however, Smith & Davis could show here, that the resulting surface mode of instability is a hydrodynamic one. Thus the Reynolds number R rather than the Marangoni number Ma is the appropriate parameter to use to characterize this instability. The results of this analysis also apply to the thermocapillary layer under certain limits; for large R, the stability of the thermocapillary layer is determined by

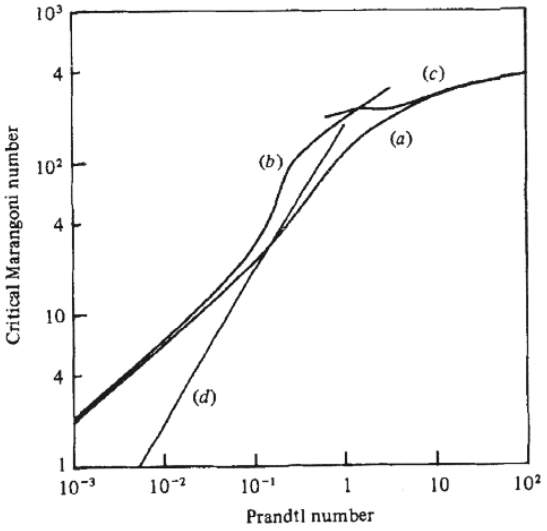


**Fig. 1.** Critical Marangoni number for the return flow in a thin liquid layer. Curve (d) is an estimate for two-dimensional surface waves in a slot with aspect ratio A = 0.1 and S = $10^4$ (Fig. 12 from Smith & Davis [2]). Curve (a) is for oblique HTWs, curve (b) is for longitudinal HTWs and curve (c) is for two-dimensional HTWs. For Pr between 1 and 10 and $Ma_{crit}$ above 4 $10^3$ some of these instabilities could coexist.

the stability of the isothermal layer. The authors then analyse the linear flow problem in the same way. They solve the eigenvalue problem for Pr between 0 and 10, S between $10^3$ and $10^4$ and for all Biot numbers B=h d/$\chi$ ( heat transfer coefficient h and the thermal diffusivity $\chi$).

The minimum of the neutral curve for Pr = 0, B=0 and S=$10^4$ for the thermocapillary layer with linear flow is around a wave number $\alpha$ =$2\pi/\lambda$ =2 and for R just below 4 $10^2$ (Fig. 1 in S&D). This minimum of the critical curve, defining the critical Reynolds number $R_c$ and a critical wave number $\alpha_c$ is rather wide and its variation with Pr and, especially with B is rather small. The largest variation occurs for S=$10^3$ and is less than 6.7% for Pr = 10 and B = $\infty$. The variation is less than 2% for S = $10^4$ and with the same changes in Pr and B. The largest variation in the critical wavenumber $\alpha_c$ is 5.7%, occurring for S = $10^5$, Pr = 10 and B = $\infty$. The largest variation in the critical phase speed $c_{Rc}$ is 4.7% occurring at the same S = $10^3$, Pr = 10 and B = $\infty$. With B = 0 the changes in $R_c$, $\alpha_c$ and $c_{Rc}$ as functions of Pr for various values of S are also very week. This lengthy discussion is needed to show the rather small variation of the neutral curve when changing Pr, B or S and this in turn is important for an application of the theoretical results to our experimental ones in spite of differences in these parameters.

Smith & Davis extended their results for various values of S, Pr and B from the linear flow to the thermocapillary layer with return flow (Figs. 7, 8 and 9 in Smith & Davis [2]). The computed neutral curves display a critical wavenumber $\alpha$ =0 of the instability for the return flow with S = $10^4$, Pr = 1 and B = $\infty$. However, all possible experiments on the instability of the thermocapillary return flow are naturally done with layers of finite length L (with end walls). The end-walls will tend to stabilize those disturbances whose wavelength is larger than the distance between the end walls. Therefore, Smith and Davis extended their analysis to larger wavenumbers $\alpha$. The results for the larger Pr presented by the authors is for Pr = 1, shown in Fig. 9 in S&D. The minimum of the critical curve is around (Re = $10^2$, $\alpha$ = 0.25) for S = $10^4$

and around ($Re = 7\ 10^2$, $\alpha = 0.45$) for $S = 10^3$. The minimum of the neutral curves for S between $10^3$ and $10^4$ is rather flat. This means that the instability can set in for a larger range of wavenumbers (what means for smaller wavelength) with only a small increase of Ra above $Ra_c$ (or Ma above $Ma_c$). It is possible that the horizontal extension of the experiment could select the critical wavelength. We can draw this conclusion because the results of Smith &Davis are rather insensitive to changes in Pr and B (at most 7% over a large range of Pr and B).

The effects of stabilization of gravity for $\alpha \to 0$ discussed by Smith & Davis do not apply to our case of a liquid layer of finite length. We can expect damping of all $\alpha$ with $\alpha \leq 2\pi A$. The analytical results of Smith & Davis are only valid for $\alpha < A^2 < 2\pi\, A$. Only by extending these results to large values of $\alpha$ through numerical computation, they can compute instabilities with larger $\alpha$ in experiments that are only weakly affected by the presence of end-walls. The end-walls are expected to damp out those disturbances whose wavelength is larger than the length L of the layer bounded by the end-walls. The corresponding neutral curves would have a non-zero minimum unlike those shown in Fig. 9 from S&D. The authors estimated the new minimum by using the R from their neutral curves that corresponds to a wavelength whose wavelength equals the layer length L, i.e. for $\alpha = 2\pi A$. The resulting estimates of the critical Marangoni number versus Pr for B=0 are given in Fig. 1 under the assumption of $A = 0.1$ and $S = 10^4$. Their crude estimate shows that SWs are preferred over oblique hydrothermal waves in a limited layer when $Pr < 0.15$. It can be expected from Fig. 1 that SWs can coexist with oblique HTWs at supercritical Ma when $Pr = 10$, where the HTWs are the preferred mode. The prediction is not so clear for $Pr = 1$ when considering two-dimensional hydrothermal waves; here the SWs could be preferred over the 2-D HTWs. Two-dimensional HTWs could be preferred over oblique HTWs in thermal boundary layers or liquid menisci at the bounding ends of the layer. There is an interesting remark at the end of the paper by Smith & Davis: "Further estimates for slightly larger $A = dL^{-1}$ and fixed S indicate, that increasing A stabilizes the flow (and lowers the value of Pr at which SWs become preferred)". We conjecture that this effect of an increase of A will occur for constant Pr when SWs are present. It can be also conjectured that SWs cannot be found in thicker liquid layers though they exist in thin liquid layers at else unchanged conditions.

### 2.1 Summary of the theory for application to the present experiments

The surface tension numbers in our experiments with ethanol are S (d = 1.0 mm) = $5.73\,10^3$ and S (d = 3.0 mm) = $5.16\,10^4$ (see Table 1). The Prandtl number is Pr = 17. The "slot length" L is equivalent to the width of the annular gap $\Delta R = 20.0$ mm (which is the space for 2D-travelling waves) and the cross stream-extension of the layer can be taken as $2\pi R = 125.66$ mm (which is the space for 2-D oblique travelling surface waves). Smith & Davis make predictions for two-dimensional surface waves but it can be estimated that the oblique travelling surface waves have nearly the same properties with a somewhat smaller critical Marangoni number.

The instabilities found in the return flow will be affected (damped) by the presence of slot ends. Damping effects occur for $\lambda > d\,A^{-1}$. We estimate for a layer with 1 mm thickness a critical Reynolds number $Re_c \approx 10^2$ and $\alpha_c \approx 0.3$, though we must take the values for $Pr = 1$ instead of those for $Pr = 17$. It can be guessed, that $Re_c$ could be one order of magnitude larger for this higher Pr; a critical Marangoni number $Ma_c \approx 10^3$ for the two-dimensional surface waves (2-D SWs) can be estimated for $Pr = 17$ from Fig. 1. The 2-D SWs are the preferred mode for $Pr \leq 0.15$ whereas the oblique hydrothermal waves are preferred for $Pr > 0.15$. For $Pr \leq 1.5$ the 2-D SWs are preferred over longitudinal HTWs and over 2-D HTWs. Whether surface

waves or hydrothermal waves are preferred, depends on the restriction of the HTW, to allow for oblique or for longitudinal or 2-D HTWs. Moreover, oblique SWs could appear at lower Marangoni number and could be preferred over HTWs for Pr = 17 under certain conditions. Finally, we do not expect SWs to appear in thicker liquid layers thought they exist in the thinner layers. The existence range of SW is limited to small A.

## 3 Experiments on surface waves in thin layers in annular gaps

### 3.1 Experimental details

The physical data of the used liquid (ethanol) are given in Table 1. The construction of one of the annular gap-experiments is sketched in Fig. 2. The optical shadowgraph-technique for the visualization of the surface waves is described in [Fig. 4 from 16].

Both experiments are with shallow annular gaps filled flat (no liquid meniscus) with ethanol. Ethanol is rather volatile at room temperature what makes provisions (a tight lid) unavoidable to reduce evaporation. Heating is from the inner wall and the cooling is from the outer wall. Figure 2 presents a sketch of the experiment A with $R_o = 77.00$ mm. The cooling is not only from the side in this experiment A but as well from the bottom. This is a boundary condition which is different from theory [2] and might pose problems of applicability. However, this design allowed temperature differences $\Delta T$ up to 40K over 20 mm in the volatile ethanol-layer and to achieve the radial temperature gradients needed for the onset of the instabilities of thermocapillary flow and, to produce the large surface oscillations of the SWs (Figs. 7, 9 and 17 in [16]). The temperature gradient is confined to a region near to the heated inner wall but extends almost 20 mm out (flow induced) and the radial temperature drop is almost linear as shown by measurements of the surface temperature in Fig. 3.

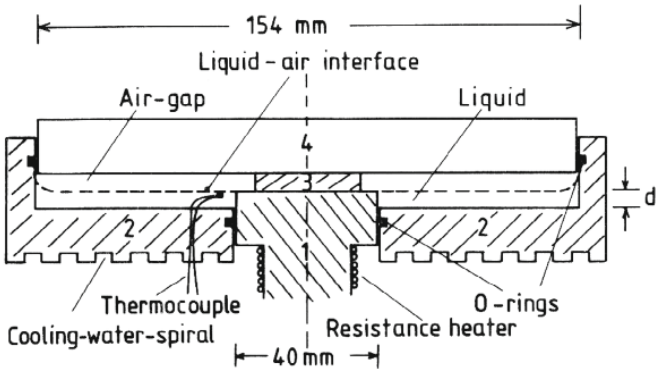


**Fig. 2.** Sketch of the **experiment A** on SWs in annular liquid layers of variable depth d heated from the inner wall and cooled from the outside wall and cooled from the bottom (isothermal bottom (2)) [16]. The free liquid surface (broken line) is under a thin air-gap (defined by a distance piece (3) positioned on the heater). The vessel is tightly closed with a plate from quartz glass (4) to avoid evaporative losses. The liquid meniscus at the cold outer wall is away from the region of interest near the hot wall, where the SWs are observed. The filling of the annular gap of experiment A and B to almost the height of the inner heater to avoid a liquid meniscus was important because underfilling resulted in strong changes of the measured critical Marangoni number [21] and in a distorted picture of the free surface.

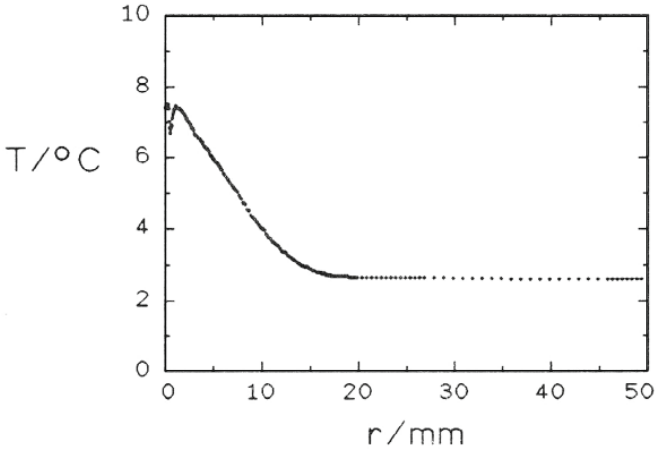


**Fig. 3.** Relative radial temperature profile near the hot side as measured with a fine thermocouple in the liquid. The thermocouples are hooked with their tips from below towards the free surface. The flow-induced "linear" radial temperature profile extends 15 mm to 20 mm away from the hot wall; d = 2.4 mm, $T_{hot}$ = 18°C, $T_{cold}$ = 2.6°C (Fig. 19 from [16]).

**Table 2.** Details and comparison of the investigated experiments and of the theory by S&D.

| | Experiment A | Experiment B | Theory by Smith&Davis | **Underfilled cuvette** |
|---|---|---|---|---|
| Geometry | Annular gap, with inner diameter=40 mm | Annular gap with inner diameter=40 mm | ∞- extended layer | **rectangular** |
| Extension of gap, dimensions | L=52 mm | L=20 mm | ∞ | **L=20 mm Width=41 mm Depth=20 mm** |
| Liquid depth | 0.5-5.0 mm | 0.6-5.0 mm | ----- | **typically 19 mm** |
| Thermal boundary conditions | Heated from the inner wall. Isothermal cold bottom | Heated from the inner wall. Thermally insulated bottom | constant temperature gradient along free surface. Insulated bottom | **Heated from the left side, cooled from the right side** |
| **Shape of free surface** | **Almost flat, no liquid meniscus** | **Almost flat, no liquid meniscus** | **Fixed flat free surface** | **Meniscus with height h=1.2 mm, pinned to upper rim** |

This gives a chance to apply theory [2] where a constant temperature gradient along the free surface is assumed.

The second experiment (experiment B) in the same way but has an adiabatic bottom in accordance with theory [2]. It has as well $R_i$ = 40 mm but a smaller annular gap of only 20 mm [21]. However, the possibility of a damping of the waves in the shorter gap is given. The features of the investigated configurations are summarized in Table 2.

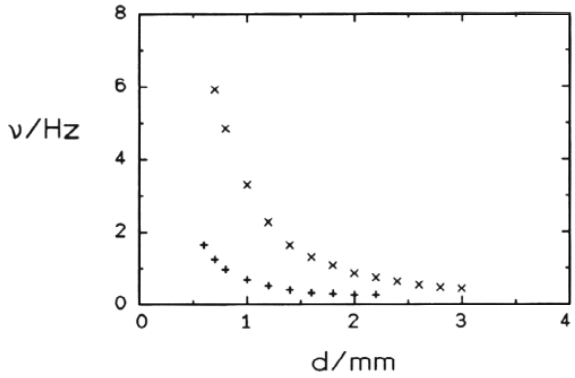


**Fig. 4.** Critical frequencies of the HTW (+) and of the SW (x) over liquid depth d (from [16]). The two instabilities can obviously coexist near above the threshold.

The wavy states are detected by their temperature oscillations with up to 3 strategically placed fine thermocouples and evaluated by Fourier analysis and correlation analysis. The thermocouples are self-made from naked NiCr-Ni-wire with a diameter of 0.05 mm or 0.025 mm (see Fig. 14). Another method was shadography with the light reflected from the free surface, recorded by a video camera and described in more detail in [16,21]. The latter method is more demanding than measurements with thermocouples or shadowgraphy with light transmitting the layer. Our method is only possible for rather flat liquid surfaces. However, this method is highly sensible for the surface deformations of the SWs.

### 3.2 Experimental results on surface waves in thermocapillary annular gaps

Figure 4 shows the critical frequencies as measured in experiment A [16] and verified in experiment B. The frequencies of both instabilities are incommensurable for all liquid depth d and increase strongly with decreasing d. The frequencies of the SWs are well above of the frequencies of the HTWs. Both waves coexisted at supercritical Ma in the range $0.6\,\text{mm} < d < 2.2\,\text{mm}$. The HTWs do not exist for $d > 2.2\,\text{mm}$ and above $d > 4.2$ no temperature oscillations by waves have been detectable at all [21]. This is in accordance with the expectations of Smith & Davis. The SWs are identified by optical observations of their approximately ten times larger surface deformations compared to that of the HTWs, by their larger wavelength, by a frequency much larger than that of the HTWs and by a critical Marangoni number different from that of the HTWs. The identification of another type of wave besides the HTW is unquestionable because we could observe and measure both waves existing at the same time under the same experimental conditions.

Almost all of the papers in literature report on temperature oscillations which are due to instabilities of the type of hydrothermal waves. Thermocapillary surface waves have been identified only in two experiments A and B [16,21].

It is time to mention that in all experiments on thermocapillary-driven instabilities the so called "steady multicellular flow structure" (also called "multirolls") is observed before the onset of the wavy instabilities and that the multicellular structure is observed to oscillate at higher driving forces as coupled to the HTW or to the SW [16,21,24]. The multicells are aligned with their axes perpendicular to the basic thermocapillary flow, in which they are embedded, and they all have the same sense of rotation. The "multicells" resemble the so called "cat-eyes" which develop between two sheering layers of the same density flowing in opposite direction. It is not clear

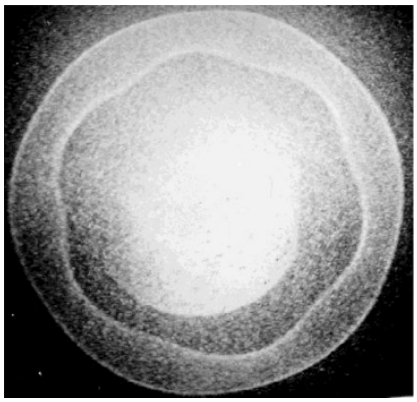

**Fig. 5.** Shadowgraphic picture (in reflection of the light from the liquid surface) of surface waves (mode m = 6) at d = 3.1 mm and $\Delta T = 24$ K in **experiment B** [21]. The 6-fold pattern rotates in such a way that an azimuthally fixed thermocouple indicates the frequency of the SWs in Fig. 4. The wavy white line lies near the heated inner cylinder. Due to a small underfilling we have a week surface depression which is focusing the illuminating light. The white "circle" of this focussed light is modulated by the azimuthally travelling SW. The outer perfect circular white line marks the outer cold limitation by a small liquid meniscus without wave. The white inner patch is from light reflected by the metallic distance piece between inner heated cylinder and the cover from quartz glass.

whether the multicellular instability is an important ingredient of the wavy thermocapillary instabilities or whether the oscillation of the multicells is only passive. We assume in the light of the theory of S & D that the multicells do not play a major role for the surface waves in the surface flow and that their oscillatory motion is passive. However, the existence of the multicells before the onset of the wavy thermocapillary instabilities is an obvious difference between theory and experimental observations; theory assumes an undisturbed return flow whereas in reality we have the multicells below the surface flow. The minimum conclusion to be drawn from this is a difference between the theoretical geometric liquid depth d and a smaller depth d′ in which the wavy instabilities of the HTW or the SW can develop. This has consequences for the value of the critical parameters of the HTWs and the SWs. We found obviously a different instability from that of the HTWs and both instabilities do develop not in the parallel return flow as assumed by S & D but in flow with cat eyes between surface flow and return flow.

The direct observation of the SWs by a shadowgraph technique (Fig. 5) and the measurement of the deformation of the surface by a travelling SW (Fig. 6) give further evidence that the waves with higher frequency are different from the HTW. The wavelength of the SW is generally larger than that of the HTW (Fig. 7), though the difference is not dramatic in the d-range where they coexist. One must note that the wavelength $\lambda$ (and the azimuthal mode number) can change dramatically when increasing Ma ($\Delta T$) what makes a measurement of $\lambda$ in case of the SW very difficult and explains the scatter in Fig. 7. The scatter of the phase speeds of the SWs is again larger than that of the HTWs (Fig. 8). However, the phase speed of the SWs is significantly larger than that of the HTWs.

The critical Marangoni numbers, from both experiments are given in Fig. 9. The values from both experiments coincide quite well (assuming a gap width L = 20 mm in experiment A). This indicates that the isothermal cold bottom of experiment A has no big influence on the SW as expected from its hydrodynamic nature. The critical Marangoni numbers in Fig. 9 show that the more dangerous mode for d $\leq$ 1.4 mm

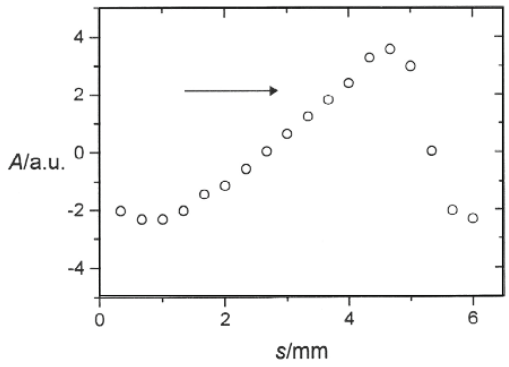


**Fig. 6.** Asymmetric surface deformation by an azimuthally travelling SW in arbitrary units for d = 1.2 mm and $\Delta T = 24$ K (from [31]). The wave travels from the left to right. The distance s is taken at the circumference of the inner cylinder. The asymmetry of the wave is considerably smaller for $\Delta T = 18$ K. The absolute value of the surface deformation by the SW lies between 5 $\mu$m and 10 $\mu$m [16] and depends on Ma whereas that of the HTWs is less than 1 $\mu$m [16].

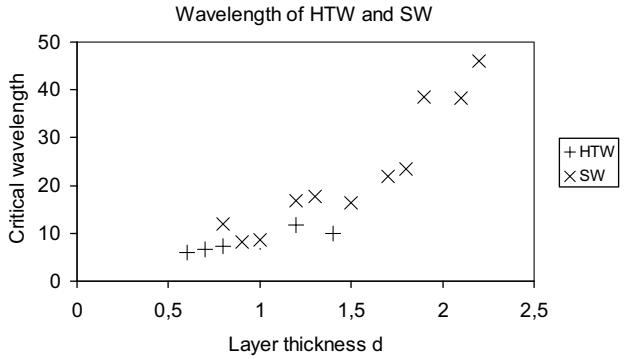


**Fig. 7.** Comparison of the wavelength of the SW with that of the HTW after experiment **A**, and after experiment **B** [16,21].

(aspect ratio A $\leq$ 0.07) is the HTW whereas the SW is the more dangerous mode for A $>$ 0.07. In the range A $\leq$ 0.15 both waves can coexist as indicated in Fig. 9. The values of the critical Marangoni numbers in Fig. 9 are in the range predicted by S&D.

Figure 10 shows an example of the optically distorted free surface of the annular gap in experiment B in shadowgraphic interferometric reflection. The HTW modulates the region near the outer meniscus at the cold side (outer white line) whereas the SW modulates the meniscus-region at the hot inner side (inner white line). The phase speeds of the two waves are rather different (Fig. 8 and figure caption of Fig. 10) with the higher phase speed of the SW.

We stress the fact that all features assigned by us to the SWs differ considerably from those of the HTW identified in [16] and [24].

The comparison between the experimental data of the SW in [16,21] and the theoretical predictions by Smith & Davis [2] is not straight forward because of the restriction in horizontal extension in the experiments compared to infinite extension in theory. Theory dealt with wavenumbers $\alpha \to 0$ whereas our wavenumbers are

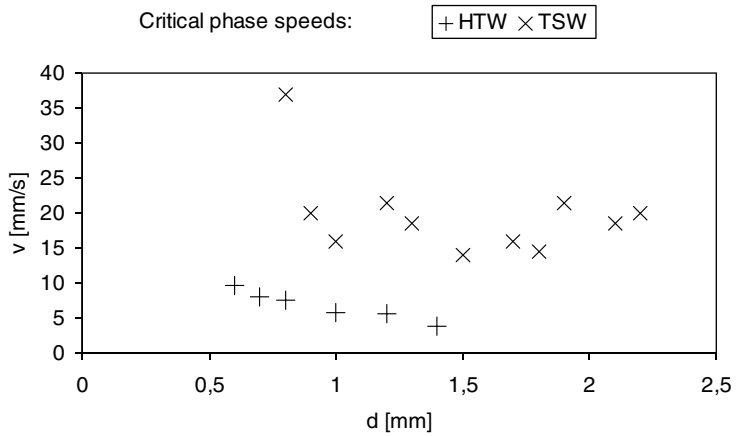


**Fig. 8.** Phase speeds of the SW and of the HTW at slightly supercritical Ma.

restricted to $\alpha > 2\pi$ A and the value of the radial wavenumber $\alpha$ (radial) can be taken as $2\pi$A, with the rather small aspect ratio A of our gap.

We see in Fig. 5 mainly an azimuthally travelling wave, in this case with six wavetrains and we could assign an azimuthal wavenumber $\alpha$(azimuth) $= 2\pi$ A. The value of the wavenumber, selected by the geometry is not very important for the value of the critical Marangoni number because the critical curve in Fig. 2 in S&D is rather flat. We estimate from this figure for d = 1 mm and S = 5 $10^3$ the critical Reynolds number $Re_c = 10^2$ and a critical wavenumber $\alpha = 0.3$. We have $Ma^c$(theory) = Pr Re = 17 Re = 1700. This compares well with the two experimental values from d = 1.0 mm, $Ma^c$ (exp) = 1560 from experiment A and $Ma^c = 1796$ from experiment B. Further insights and their limitations are formulated in the discussions in [21]. The non-linear character of the SW is expressed in experiment B as intermittent behaviour [21] in accordance with a non-linear theory of the SWs [32]. This is again a hint that we dealt with SWs in the experiments A [16] and B [21].

### 3.3 Why have the surface waves not been observed in other experiments on thermocapillary flow?

We found the following optimum conditions for the appearance of thermocapillary surface waves in the annular slot experiments:

1. Small layer thickness of the order of 1 mm.
2. Lateral extension of the order of 20 mm and more.
3. Azimuthal geometry with large azimuthal extension $2\pi$R (20 mm $\leq$ R) for the waves to travel cross-stream (as observed).
4. Prandtl number Pr < 20.
5. Reduced evaporative loss for constant filling of the annular gap.
6. Flat filling of the gap because the critical Ma increases with underfilling.
7. Vibration-insulated mounting of the annular gap with its large free surface.
8. Dimensions larger than in [16,21] would run into difficulties because of large evaporation and, because of boiling of the liquid at the hot side to reach the critical Marangoni number ($\Delta$T critical).

One experiment in which SWs could have been observed is [24] but this was not reported there. The Prandtl number used in this work was approximately Pr = 14, the extension of the layer was large enough and the liquid depth was small enough.

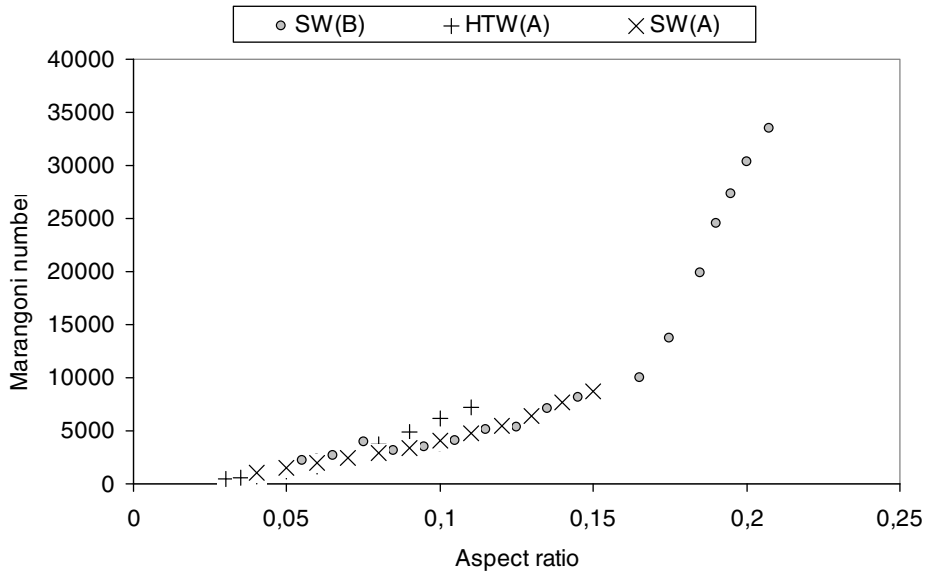


**Fig. 9.** Critical Marangoni numbers $Ma^c$ of the SW and of the HTW adopted from experiments A and B [16,21]. The differences between the HTW and the SW are more clearly visible when plotting the critical temperature difference over layer depth d as in [16]. The critical Marangoni numbers from experiment A [16] for A = 0.05 (d = 1.0 mm) are $Ma^c$(HTW) = 1190 and $Ma^c$(SW) = 1560. For A = 0.1 (d = 2 mm) the authors of [16] report $Ma^c$(HTW) = 6150 and $Ma^c$(SW) = 4040. The critical Marangoni numbers of the SW from experiment B [21] are comparable to those from experiment A with the tendency to somewhat larger values for smaller A. The cold isothermal bottom in [16] seems to play no role for the value of $Ma^c$.

A reason for missing the SWs could have been the sidewalls in the rectangular configuration used in this work which would damp the cross-stream travelling waves–in contrast to the annular configuration. The main reason of the authors of [24] to miss the SWs was probably the use of an IR-camera to detect the waves. Such a camera is sensitive for the temperature oscillations of the HTWs but not for the surface oscillations of the SWs.

The Prandtl number of the 5cSt-silicone oil used in [19] was too high and the liquid depth at the higher limit. The latter is true for most other experiments in annular gap configuration or rectangular liquid layers [15,27–29], however, the authors of [29] and their group work with silicone oil of Pr = 10 and in annular gaps with the requested thin layers and could have observed SWs. They observe much more types of waves than pure HTWs (see Fig. 5 in [29]). They interpret and model their results in the framework of theory of nonlinear waves, e.g. in one case as secondary Eckhaus instability. Another reason for the authors of [29] and this group not finding SWs could be the difference in Prandtl number and in surface tension parameter S. However, we conjecture that these authors miss the surface deformation by the SWs because they used a shadographic technique based on light transmitting the liquid layer. Their method is most sensitive to thermal disturbances and thus on HTWs, whereas we used shadowgraphy with light reflected from the free surface, which latter method is most sensitive to surface deformations.

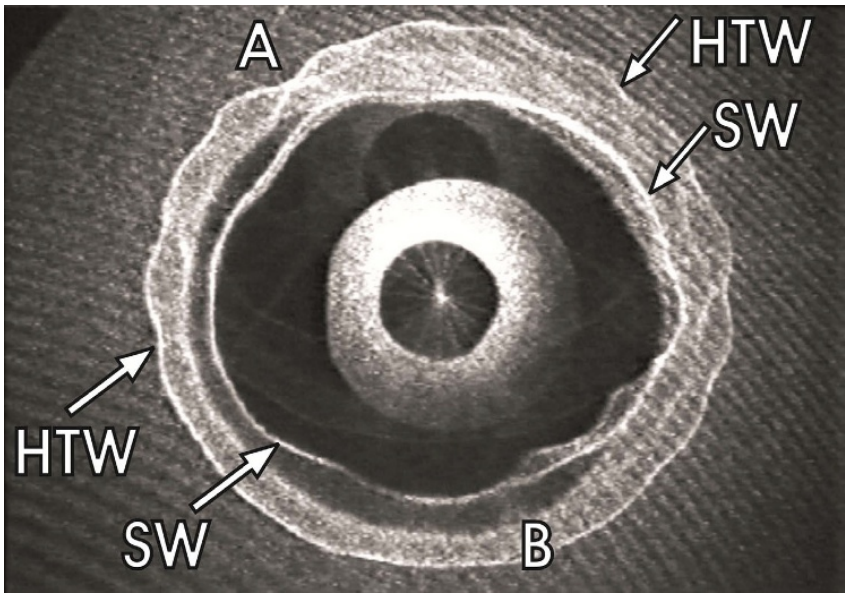


**Fig. 10.** Shadowgrapic-interferometric picture of light reflected from the free surface of the annular gap. The HTW (outer white line with approx. 16 wavetrains on 360° is travelling from point A (source) azimuthally in both directions, interfering in range B (sink). The SW modulates the meniscus at the inner hot meniscus with approximately 7 wavetrains. It seems to travel counter clockwise to the HTW. The annular gap of 20 mm width appears smaller than the radius of the inner cylinder (diameter 40 mm) because it acts as a concave mirror due to slight underfilling. The phase speed $v_\varphi$ of the SW in this example is approximately 60°/s and thus much higher than that of the HTW with 6°/s.

A type of hydrothermal wave has been investigated very often in liquid bridges. Liquid bridges, however, are only a few millimetres long and in most cases to thick with 5 to 6 mm in diameter. The small length as well as the small circumference will prevent the development of SWs. The only experiment with a 15 mm long liquid bridge was executed under microgravity. But the Prandtl number was as large as 28 and, 15 mm length are probably not sufficient and the highest applied temperature difference was only 12 K. In a rough estimation one could compare the radius of the liquid bridge (e.g. r = 3 mm) to the liquid layer depth d and sees that the "liquid depth" of the liquid bridges is in the higher limit for SWs to occur.

## 4 Standing surface gravity waves excited by surface waves in the cold liquid meniscus of a side-heated underfilled cuvette

The phenomenon of standing gravity surface waves (SGSWs) in thermocapillary-driven flow was observed by chance some time ago by Metzger [33] whereas its nature was revealed later by Bach [26]. The SGSW was observed in experiments with a side-heated rectangular cuvette of e.g. L = 20 mm, W = 41 mm, D = 20 mm which was originally filled up to the rim (no liquid meniscus) with ethanol to study buoyant-thermocapillary convection. After enough loss of the ethanol due to evaporation the cuvette was underfilled and a free surface with a liquid meniscus at the sidewalls was formed. At a certain level of underfilling the SGSWs have been observed. They have

a frequency of the order of 7 Hz in this cuvette and a peak-peak amplitude of up to 1 mm. The distance between the thermostated copper-endwalls of the cuvette is L, the temperature difference is $\Delta T$.

We will now demonstrate in the following step by step;

1. Standing gravity surface waves occur for sufficient large temperature difference $\Delta T$ in a certain range of under-filling.
2. Themocapillary flow with return flow separates from buoyancy-driven flow in the bulk liquid. Thermocapillary further develops a "separated region" in the cold liquid meniscus.
3. HTWs and SWs develop in this separated meniscus. Parts of the frequency spectrum of HTWs and of SWs in this meniscus region match the possible frequency spectrum of SGSW in the free liquid surface of this cuvette.
4. The most probable resonant excitation of some SGSWs is by the third harmonics of a SW in the meniscus.
5. We will demonstrate the resonance mechanism by tuning the frequencies of the oscillations in the meniscus to that of the SGSWs. We could as well detune the resonance by changing the cuvette dimensions.

This example with the thermocapillary instabilities in the liquid meniscus shows that the existence of the SWs is not limited to the more academic case of thin liquid layers.

### 4.1 Standing gravity surface waves in a rectangular cuvette–the influence of under-filling and the general spectrum of SGSWs in this geometry

A cuvette of 20 mm depth, underfilled with ethanol by typically 1.0 mm, heated from the one end and cooled from the opposite one shows standing gravity surface waves when a certain temperature difference between the ends is exceeded. These oscillations do not occur if the cuvette is completely filled (no meniscus), or if the underfilling is so large that the meniscus is no longer pinned to the sharp rim of the cuvette-ends. Figure 11 shows the frequency of the surface oscillations measured by a thermocouple in an optimum position with its tip near the free surface to detect SGSWs. The oscillating surface has points of maximum amplitudes (crests) and of minimum amplitudes (nodes) as normal for standing waves. The oscillations have a sharp frequency peak and higher harmonics are clearly visible.

The spectrum of SGSWs in an underfilled rectangular cuvette can be calculated only approximately. We excited SGSWs independently from the excitation by oscillations in the cold meniscus by short shocks of the table and we visualized them by shadowgraphic pictures of light reflected from the free surface to have an overview. In a first approximation we have $\lambda_n = 2L/n$, $\lambda_m = 2\,W/m$, $\lambda_{k,l} = 1/((k/4L)^2 + (1/4W)^2)^{1/2}$, with the frequencies of standing gravity waves (SGWs) $f_n = (ng/\pi L)^{1/2} \ldots$ etc. The reader can refer to [36–38] for further details of SGSWs in rectangular containers.

By thermocouple measurement we could identify the oscillation mode $n = 1$ (basic mode along the temperature gradient/x-axis) with $f = 7.22$ Hz; $m = 2$ (first harmonic along the y-axis with $f = 7.22$ Hz); $k = 1$, $l = 1$, basic diagonal oscillation with $f = 4.68$ Hz; $k = 2$, $l = 2$, first harmonic diagonal with $f = 9.22$ Hz.

The surface oscillation amplitude (e.g. for mode $n = 1$ in Fig. 12) shows a steep increase at an underfilling $h = 0.45$ mm and its corresponding meniscus shape. The surface oscillations cease again for an underfilling around $h = 1.8$ mm. This underfilling is the point when the meniscus contact line changes from being pinned to the sharp upper edge of the end-wall to a meniscus with "free slip contact line". We assume that the condition of "free slip" suppresses the SWs. It will change the spectrum of possible SGSWs, anyhow.

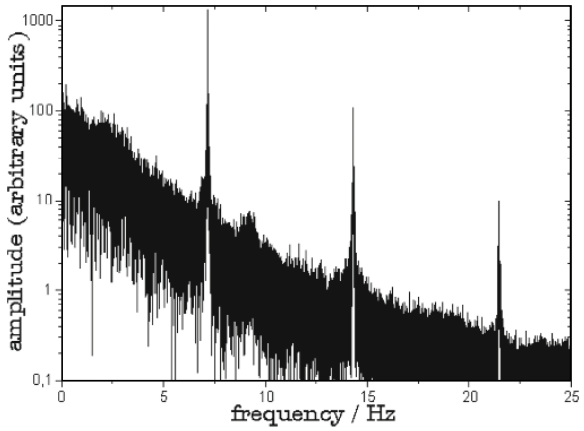


**Fig. 11.** Fourier analysis of the surface oscillations of the SGSWs excited by oscillations in the meniscus at the cold wall. The main frequency is about 7 Hz with its 3rd harmonics at around 21.3 Hz.

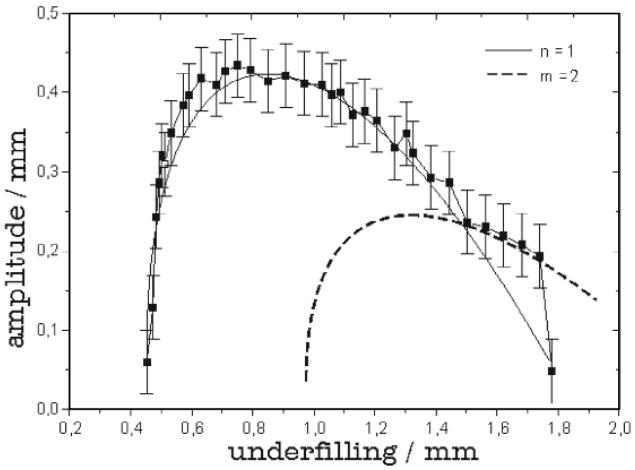


**Fig. 12.** The maximum amplitude (in millimetres) of the surface oscillations of two different modes of the SGSWs depends on the under-filling h of the cuvette (on the meniscus-height h).

We have menisci at the hot and at the cold end and the question arose whether the oscillations that excite the SGSWS come from the hot meniscus or from the cold one. This question was answered by slightly tilting the cuvette around the y-axis through its centre, to increase or to decrease the meniscus height at will at the cold or at the hot end under constant temperature gradient for the appearance of the SGSWs; the surface oscillations arose only under the "under-filling conditions" at the cold side. The liquid meniscus at the cold side is the location of the exciting oscillations.

In order to distinguish between hydrodynamic instabilities and surface oscillations we changed the cuvette dimensions in some cases to change the frequencies of the SGSWs drastically (e.g. we changed to L = 16 mm or to L = 12 mm, or changed to W = 35 mm. This allowed us to measure possible exciting hydrodynamic oscillations in the menisci without the resonance with the SGSWs.

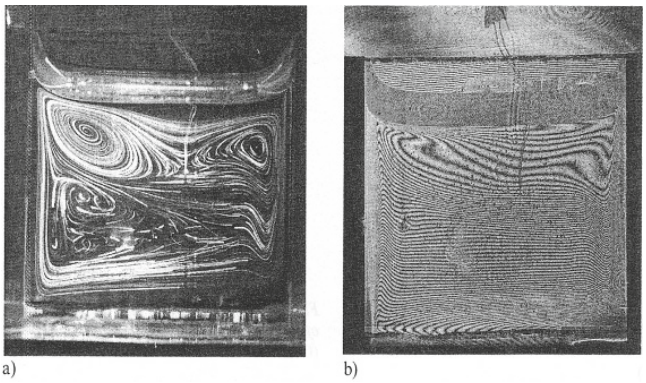


**Fig. 13.** a) Left: streamlines by tracer streaks and b) right: isotherms by holographic interferometry in a strongly under-filled cuvette (20mmx20mmx41mm), heated from the left and cooled from the right [35]. Reflection pictures and a thermocouple are visible above the free surface. We observe a flow-dominated temperature field with a rather homogeneous temperature in the thermocapillary convection with its return flow (Fig. 13b).

Very important is the observation of the existence of a critical temperature difference $\Delta T$ between the copper ends for the onset of the SGSWs, obeying the law of a Hopf-bifurcation (Fig. 16). We draw the conclusion from it that the excitation is by a hydrodynamic phenomenon. The reader is referred to the thesis of Ch. Bach [26] for further details.

### 4.2 Thermocapillary flow with its return flow separating from buoyant flow and further separation in the cold liquid meniscus

It was observed for ethanol and for liquids with comparable Prandtl number that a hotter thermocapillary-driven surface flow on top separates from the colder buoyancy-driven flow underneath [34,35]. This is demonstrated by streak-lines and by isotherms in Fig. 13.

### 4.3 The liquid meniscus at the cold end-wall and surface waves

When the cuvette is underfilled a further separation of the region in the cold meniscus occurs. Figure 14 shows a medium under-filling with a well developed liquid meniscus. The separated meniscus-area with a separated convection roll in the upper corner is clearly visible. One part of the surface flow coming from the left hot side streams further along the free surface whereas the bigger part flows downward with higher velocity; we call this scenario "separation of a vortex at the cold wall". This scenario develops more and more in this direction the higher the meniscus becomes. For an under-filling $h = 1.8\,mm$ one can observe up to 4 separated convection rolls in the wedge-shaped meniscus, all of different extension, depending on their position.

The situation is somewhat similar to that of the multicells in front of the cold wall in a thin side-heated liquid layer. We can assume the existence of two-dimensional HTWs and SWs in this narrow meniscus region. The situation is much more complex

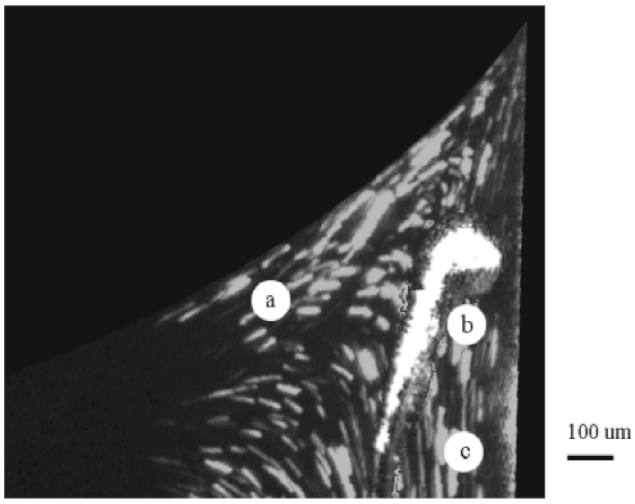


**Fig. 14.** Flow visualisation by tracer streak lines in a vertical light cut, h ≈ 1.2 mm and different possible positions for the thermocouple-tip (red marked) to detect different signals. The bright golf club-like reflection is from the LASER-light sheet from a naked fine thermocouple wire.

because the wedge-shaped meniscus allows for multirolls of different size. However, as pointed out earlier, we can assume that HTWs and especially SWs are not coupled to the underlying convection rolls. The surface oscillations by these waves could excite SGSW in the free surface of the liquid (Fig. 11 and Fig. 14).

It is very difficult to differentiate and to measure the exciting oscillations of the HTW and the SW on top of very large oscillations of the SGSWs which have nearly the same frequency due to their resonance relation. For measuring the SW the thermocouple must be placed near a node of the standing wave. By placing the thermocouple tip in point (a) of Fig. 14 one would catch oscillations from the free surface which are transported by flow towards the cold end-wall. Placing the thermocouple near (b) is for catching oscillations from hydrodynamic instabilities in the meniscus, transported downwards by the flow along the cold wall. Moreover, placing the thermocouple in a node of the SGSWs in cross-stream direction one can partly avoid the superposition of the hydrodynamic signal with that from the SGSWs.

We have already shown that the SGSWs are excited by a process in the meniscus at the cold end-wall. Concerning whether hydrodynamic instabilities exist in the meniscus at the hot wall, we could never detect the oscillation signals from hydrodynamic instabilities in the meniscus at the hot end. The reason for lacking instabilities in the hot liquid meniscus is the different condition for flow separation at the hot end compared to the cold end.

### 4.4 Evidence for the instabilities in the cold meniscus exciting the standing gravity surface waves in resonance

We present in Fig. 15 one example of oscillation spectra measured with an extra fine thermocouple (wire diameter 0.025 mm) positioned in the cold fluid meniscus. The strongest signals come from the exited SGWs. They are very broad, presumably by

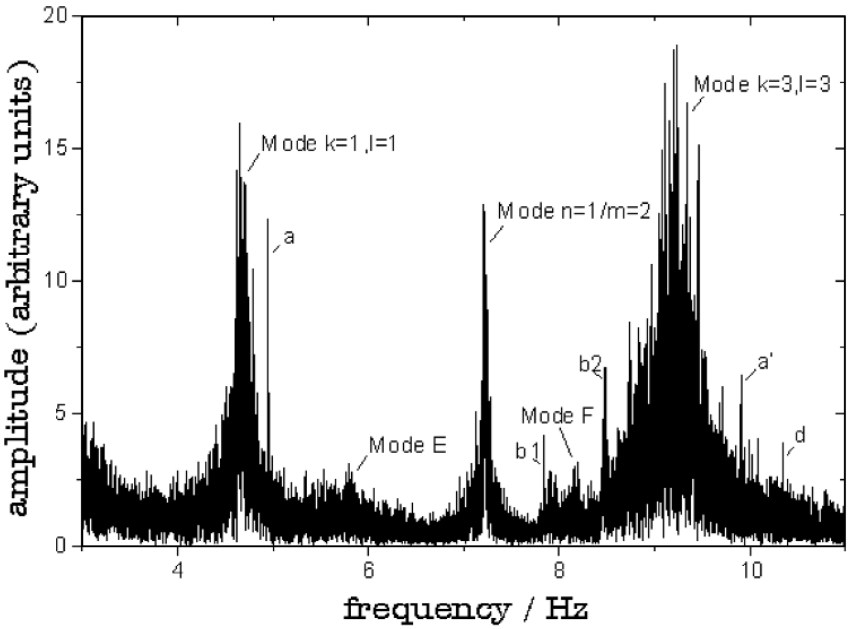


**Fig. 15.** One example of temperature oscillation-measurements aiming to detect the exiting oscillations (the sharp spikes, e.g.:"a", "b1", "b2","a′").

disturbing vibrations from the environment, by liquid-level change during the long data acquisition time for the spectrum, by reflection of the SGWSs in the four menicus regions and by possible non-homogeneities in the menisci. We could change the position of the broad frequency bands dramatically by changing the cuvette dimension. These broad frequency bands belong definitely to the surface oscillations of the SGSW. The frequencies of the broad bands fit to the frequencies calculated for SGSWs in a cuvette with L = 20 mm, W = 41 mm, filled with ethanol. They are labelled in Fig. 15 according to increasing frequency (k = 1, l = 1), (n = 1 coinciding with m = 2) and (k = 3, l = 3). Besides these broad frequency bands we could detect sharp line-like frequency peaks (Fig. 15). These sharp frequencies (e.g. at 4.95 Hz labelled "a" and its harmonics near 9.9 Hz labelled "a′" are not affected by a size-change of the cuvette and are therefore assigned to hydrodynamic instabilities in the cold liquid meniscus. Not shown in Fig. 15 is signal "d′" (harmonic of "d") with 20.6 Hz.

The frequency oscillation peaks of the SGSWs are broad enough that an exciting hydrodynamic oscillation near their half width could excite them by parametric resonance. Thus it is possible that "a" is exciting (k =1, m =1) or, that "b2" or "a′" are exciting (k = 3, l = 3). There is the possibility, that "d′" with 20.6 Hz excites the standing surface waves n = 1 and m = 2 in parametric resonance because "d′" has approximately three times the frequency of (n = 1 and m = 2). Our situation is just like this; (i) the SWs are travelling along the meniscus confined to the cold wall. (ii) They excite with their faint surface oscillations in the meniscus the free surface of ethanol. (iii) The cuvette acts as resonating system for the excited SGSWs.

Most interesting are the oscillation frequencies "d" and its harmonics "d′" which we assign to the hydrodynamic instability of the SWs. The oscillations "d" and "d′" are of hydrodynamic nature as shown by the existence of a threshold and the

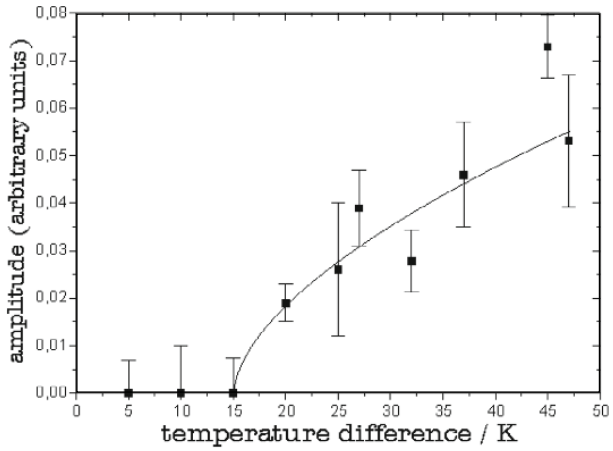


**Fig. 16.** Increase of the signal amplitude of the frequency peak "d′" with the applied ΔT. Frequency "d" is assigned to a SW in the cold meniscus (from thermocouple signals) from [26].

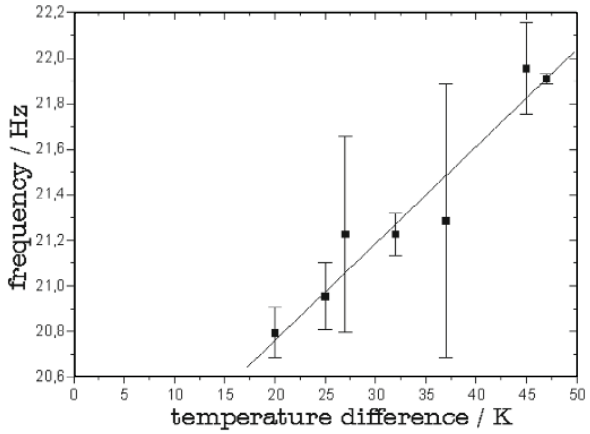


**Fig. 17.** Strong shift of the frequency peak-position of peak "d′" (hydrodynamic instability) by the temperature difference ΔT.

behaviour as a Hopf-bifurcation at the threshold when increasing the Marangoni number by increasing ΔT (Fig. 16).

One can tune or can detune the resonance between the exciting oscillations and the standing surface gravity waves. Figure 17 shows the possibility to increase the frequency of the hydrodynamic oscillation "d′" by increasing the temperature difference. The frequency of the SGSWs is rather unaffected by a change of ΔT. One can arrange perfect or not so perfect resonance between exciting hydrodynamic instabilities in the liquid meniscus and the SGSWs by adjusting ΔT or the under-filling h.

An example of this resonance mechanism is shown in Fig. 18 for the main SGSW mode (n = 1 coinciding with m = 2) with approximately 7 Hz and its most dangerous excitation mode by the hydrodynamic instability "d′" with approximately three times the frequency (21 Hz). These two oscillations can couple perfectly because of their frequency relation 3:1. The amplitude of the SGSW is largest for vanishing

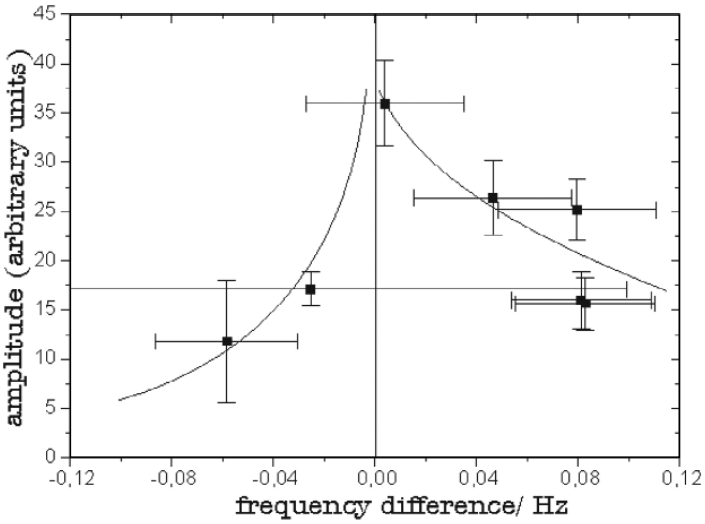


**Fig. 18.** Amplitude of the SGSW m = 2 dependent on the frequency difference to its exciting SW "d′". The amplitudes of the SGSW and that of the SW have been measured by thermocouples when changing the under-filling h ($\Delta T = 25\,K$, $L = 12\,mm$ to suppress other SGSWs except mode m = 2, $B = 41\,mm$).

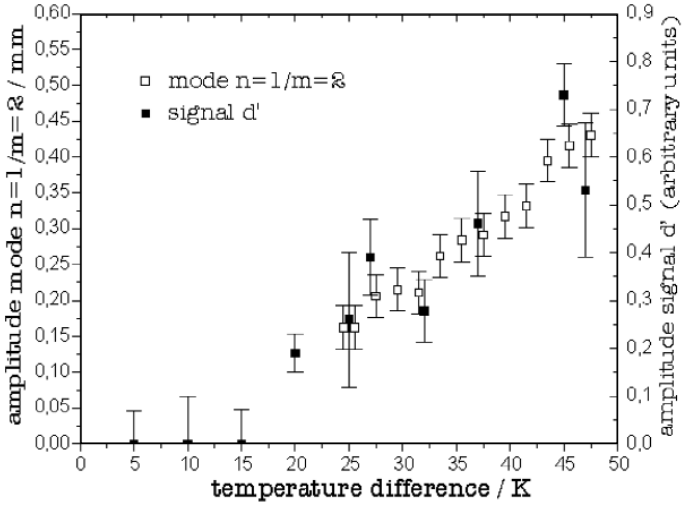


**Fig. 19.** Comparison of the ΔT-dependence of the amplitudes of the exciting SW "d′" and that of the SGSW (n = 1, m = 2). The amplitude of the SGSW was gained by measuring the surface deformations by an optical method, the amplitude of the SW comes from thermocouple measurements (normalized).

frequency difference. Figure 19 shows essentially the same amplitude-dependence of the frequency "d′" of the exciting SW and the surface oscillations of the excited SGSW n = 1/m = 2. We see in Fig. 19 that the SGSW has approximately the same threshold as the exciting SW in the liquid meniscus. This again is strong evidence for the resonant excitation of the SGSW by the oscillation "d′" in the liquid meniscus.

## 5 Conclusions

We extracted the main predictions on surface waves in thermocapillary liquid layers made by a theory [2], which considered the instabilities in infinitely extended thin liquid layers with thermocapillary flow with return flow, taking the flexibility of the free surface into account. Two-dimensional calculations predicted critical Marangoni numbers $Ma^c$ of approximately $10^2$ for liquids with Prandtl number 17. It is pointed out that the stream-wise dimension will select the wavenumber of the most critical mode. The dependence of the critical Marangoni number on the wavenumber is rather small in the range of the larger wave-numbers what allows us to estimate $Ma^c \approx 3\ 10^4$ for experiments with ethanol, where $Ma^c$ depends further on the aspect ratio of the gap. Theory [2] predicts as well the existence of hydrothermal waves in the same range of Ma what makes it possible that both instabilities could appear simultaneously and can be directly compared in experiments at supercritical Ma.

We reviewed and complemented the results of two experiments with differentially heated thin liquid layers in annular slots in which surface waves (SWs) occurred for layers with thickness d below 2.2 mm. We presented measurements of frequencies, wavelength, phase speeds and critical Marangoni numbers of the SWs for different aspsect ratios. The description is complemented by pictures of the surface deformations by the SWs. The experimental critical Marangoni numbers are in the range predicted by Smith & Davis [2]. The assignment of the experimental observations to the SWs of this theory was concluded from the observation of much larger surface deformation and from the larger wavelength and phase speed compared to hydrothermal waves. It was argued that the SWs have not been observed by other experimenters because of too small horizontal extension of their layers, or too small Marangoni numbers, or too large or differing Prandtl numbers. A further reason of other researchers to miss the SWs in their experiments could be the much smaller sensitivity for surface deformations of their detection methods compared to our shadowgraphy with light reflected from the free surface.

The observation of thermocapillary instabilities in the liquid meniscus at the cold wall of a 20 mm deep, under-filled cuvette is due to a strong separation of the thermocapillary-driven flow from the flow in the bulk liquid in this small region. This creates thermocapillary flow with return flow in a narrow wedge-shaped meniscus somehow similar to the flow in side-heated layers. We can assume a variety of thermocapillary instabilities to exist there, travelling mainly along the wall. We assume among them instabilities of the type of SWs because of the excitation of macroscopic standing gravity surface waves by these hydrodynamic instabilities. We could identify one instability which could be exciting SGSWs in parametric resonance. This thermocapillary instability in the cold meniscus behaves like a Hopf bifurcation (as do the SGSWs). The excitation of macroscopic surface waves with amplitudes up to 0.5 mm by faint surface oscillations of the SWs in the liquid meniscus is only possible by resonance and for standing waves.

Dietrich Schwabe is grateful to DAAD for the financial support (reference 521/nm) to attend the $7^{th}$ Conference of the International Marangoni Association, 23. 06.–26. 06. 2014 at the Technical University of Vienna (Austria). We thank Dr. Juergen Schneider who supplied the video for the photo in Fig. 10.

## References

1. M.K. Smith, S.H. Davis, J. Fluid. Mech. **132**, 119 (1983)
2. M.K. Smith, S.H. Davis, J. Fluid. Mech. **132**, 145 (1983)

3. F. Preisser, D. Schwabe, A. Scharmann, J. Fluid Mech. **126**, 454 (1983)
4. J.-J. Xu, S.H. Davis, Phys. Fluids **27**, 1102 (1984)
5. R. Velten, D. Schwabe, A. Scharmann, Phys. Fluids A **3**, 267 (1991)
6. S. Frank, D. Schwabe, Exp. Fluids **23**, 234 (1997)
7. K.A. Muehlner, M.F. Schatz, V. Petrov, W.D. McCormick, J.B. Swift, H.L. Swinney, Phys. Fluids **9**, 1850 (1997)
8. J. Leypoldt, H.C. Kuhlmann, H.J. Rath, J. Fluid Mech. **414**, 285 (2000)
9. D. Schwabe, Adv. Space Res. **29**, 651 (2002)
10. D. Schwabe, Phys. Fluids **17**, 112104 (2005)
11. H. Kawamura, E. Tagaya, Y. Hoshino, Heat Mass Transfer **50**, 1263 (2007)
12. S. Tanaka, H. Kawamura, I. Ueno, D. Schwabe, Phys. Fluids **18**, 067103-1 (2006)
13. D. Schwabe, A. Mizev, M. Udhayasankar, S. Tanaka, Phys. Fluids **19**, 072102 (2007)
14. E. Hofmann, H.C. Kuhlmann, Phys. Fluids **23**, 072106-1 (2011)
15. D. Schwabe, "Oscillatory thermocapillary convection in a horizontal shallow liquid layer heated from a side-wall" p. 127-128 in: Abstracts of the 5$^{th}$ International Conference on Physico-Chemical Hydrodynamics, Israel, Tel-Aviv, December 16–21 (1984)
16. D. Schwabe, U. Möller, J. Schneider, A. Scharmann, Phys. Fluids. A **4**, 2368 (1992)
17. D. Villers, J.K. Platten, J. Fluid. Mech. **234**, 487 (1992)
18. J.M. Vince, M. Dubois, Europhys. Lett. **20**, 505 (1992)
19. A.B. Ezersky, A. Garcimartin, J. Burguete, J. Mancini, H.L. Perez-Garcia, Phys. Rev. E **47**, 1126 (1993)
20. F. Daviaud, J.M. Vince, Phys. Rev. E **48**, 4432 (1993)
21. J. Schneider, D. Schwabe, A. Scharmann, Microgravity. Sci. Technol. **9**, 86 (1996)
22. C. De Saedeleer, A. Garcimartin, G. Chavepeyer, J.K. Platten, Phys. Fluids. **8**, 670 (1996)
23. E. Favre, L. Blumenfeld, Phys. Fluids **9**, 1473 (1997)
24. R. Riley, G. Neitzel, J. Fluid. Mech. **359**, 143 (1998)
25. Y. Kamotani, S. Ostrach, J. Masud, J. Fluid. Mech. **410**, 211 (2000)
26. Ch. Bach, "Resonanz von Oberflaechenwellen mit thermokapillaren Instabilitaeten in einem Meniskus", Ph.D. thesis, Justus-Liebig-Universität Giessen, 2000
27. N. Garnier, A. Chiffaudel, Eur. Phys. J. B **19**, 87 (2001)
28. J. Burguete, N. Mukolobwiez, F. Daviaud, N. Garnier, A. Chiffaudel, Phys. Fluids **13**, 2773 (2001)
29. N. Garnier, A. Chiffaudel, F. Daviaud, Phys. D: Nonlin. Phenom. **174**, 1 (2001)
30. M.D. Neary, K.D. Stepanoff, Phys. Fluids **30**, 2936 (1987)
31. J. Schneider, Strukturen thermokapillarer Konvektion in einem Ringspalt, Thesis Justus-Liebig Universitaet Giessen, 1995
32. R.A. Kraenkel, J.G. Pereira, M.A. Manna, Phys. Lett. A **185**, 88 (1994)
33. J. Metzger, "Experimente zur Kopplung von Auftriebs- und thermokapillarer Konvektion," Diploma thesis, University of Giessen, 1986
34. D. Schwabe, J. Metzger, J. Crystal Growth **97**, 23 (1989)
35. D. Schwabe, H. Duerr, Microgravity Sci. Technol. **9**, 201 (1996)
36. G.R. Verma, J.B. Keller, Phys. Fluids **5**, 52 (1962)
37. P. Bryant, M. Stiassnie, J. Fluid. Mech. **302**, 65 (1995)
38. P.D. Weidmann, J.A. Norris, Phys. Chem. Hydrodyn. **9**, 393 (1987)